

# Fluoridonitrosyl Complexes of Technetium(I) and Technetium(II). Synthesis, Characterization, Reactions, and DFT Calculations

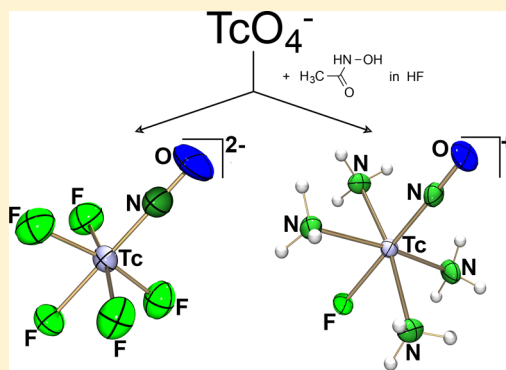
Samundeeswari Mariappan Balasekaran,<sup>†</sup> Johann Spandl,<sup>†</sup> Adelheid Hagenbach,<sup>†</sup> Klaus Köhler,<sup>‡</sup> Markus Drees,<sup>‡</sup> and Ulrich Abram<sup>\*†</sup>

<sup>†</sup>Institute of Chemistry and Biochemistry, Freie Universität Berlin, Fabeckstr. 34/36, D-14195 Berlin, Germany

<sup>‡</sup>Department of Chemistry, Inorganic Chemistry, Technische Universität München, Lichtenbergstr. 4, D-85747 Garching, Germany

## Supporting Information

**ABSTRACT:** A mixture of  $[\text{Tc}(\text{NO})\text{F}_5]^{2-}$  and  $[\text{Tc}(\text{NO})(\text{NH}_3)_4\text{F}]^+$  is formed during the reaction of pertechnetate with acetohydroxamic acid (Haha) in aqueous HF. The blue pentafluoronitrosyltechnetate(II) has been isolated in crystalline form as potassium and rubidium salts, while the orange-red ammine complex crystallizes as bifluoride or  $\text{PF}_6^-$  salts. Reactions of  $[\text{Tc}(\text{NO})\text{F}_5]^{2-}$  salts with HCl give the corresponding  $[\text{Tc}(\text{NO})\text{Cl}_{4/5}]^{-/2-}$  complexes, while reflux in neat pyridine (py) results in the formation of the technetium(I) cation  $[\text{Tc}(\text{NO})(\text{py})_4\text{F}]^+$ , which can be crystallized as hexafluoridophosphate. The same compound can be synthesized directly from pertechnetate, Haha, HF, and py or by a ligand-exchange procedure starting from  $[\text{Tc}(\text{NO})(\text{NH}_3)_4\text{F}](\text{HF}_2)$ . The technetium(I) cation  $[\text{Tc}(\text{NO})(\text{NH}_3)_4\text{F}]^+$  can be oxidized electrochemically or by the reaction with  $\text{Ce}(\text{SO}_4)_2$  to give the corresponding Tc(II) compound  $[\text{Tc}(\text{NO})(\text{NH}_3)_4\text{F}]^{2+}$ . The fluoro ligand in  $[\text{Tc}(\text{NO})(\text{NH}_3)_4\text{F}]^+$  can be replaced by  $\text{CF}_3\text{COO}^-$ , leaving the “[Tc(NO)-(NH<sub>3</sub>)<sub>4</sub>]<sup>2+</sup> core” untouched. The experimental results are confirmed by density functional theory calculations on  $[\text{Tc}(\text{NO})\text{F}_5]^{2-}$ ,  $[\text{Tc}(\text{NO})(\text{py})_4\text{F}]^+$ ,  $[\text{Tc}(\text{NO})(\text{NH}_3)_4\text{F}]^+$ , and  $[\text{Tc}(\text{NO})(\text{NH}_3)_4\text{F}]^{2+}$ .



## INTRODUCTION

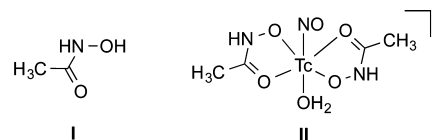
The important role of nitric oxide in biological processes or as ligands in biologically or catalytically active metal complexes is undoubted.<sup>1–4</sup> Nevertheless, there are relatively fewer studies that are devoted to the fundamental chemistry of the noninnocent nitrosyl ligand and its metal complexes. This is also true for technetium nitrosyls, which were discussed in the 1980s as potentially suitable radiopharmaceuticals for myocardial imaging.<sup>5</sup> Recently, they re-entered the focus of interest of researchers in nuclear medicine after the development of mixed carbonyl/nitrosyl complexes.<sup>6–9</sup> For further developments in all these sectors, more knowledge is required about structure, bonding, and reactivity of nitrosyl complexes. In this context, we extended our fundamental studies on technetium compounds with fluoro ligands to corresponding nitrosyl complexes.<sup>10,11</sup>

Nitrosyl complexes of technetium are known with the metal in the formal oxidation states of +1 to +3.<sup>12</sup> The linearly coordinated NO ligand is consequently regarded as a three-electron-donating  $\text{NO}^+$  species. Common starting materials for the synthesis of technetium nitrosyls are  $\text{TcO}_2$ ,  $\text{TcO}_4^-$ ,  $[\text{TcX}_6]^{2-}$ ,  $[\text{TcOX}_4]^-$  complexes ( $\text{X} = \text{Cl}, \text{Br}, \text{I}$ ) or phosphine complexes of Tc(III). They normally react with gaseous NO or hydroxylamine hydrochloride under reductive nitrosylation.<sup>13–20</sup> Only in some exceptional cases the oxidation state of the metal remains unchanged.<sup>18</sup> Other methods introduce the nitrosyl ligand into low-valent technetium compounds by reactions with  $\text{NO}^+$  salts,  $\text{HNO}_3$ ,  $\text{NaNO}_2$ , or  $\text{NO}_2$ .<sup>5,6,21</sup>

Nitrosyltechnetium compounds with fluoro ligands, however, could not be prepared by the established procedures.

Recently, a novel approach to nitrosyltechnetium complexes was introduced by the use of acetohydroxamic acid, Haha (I) (see Chart 1). The compound reduces  $\text{TcO}_4^-$  or  $\text{TcO}_2$  in

Chart 1. Acetohydroxamic Acid and Its Tc(II) Complex<sup>13</sup>



acidic media. A unique, highly hydrophilic compound is formed, which has been characterized as a cationic complex of the composition  $[\text{Tc}(\text{NO})(\text{aha})_2(\text{H}_2\text{O})]^+$  (II) (Chart 1) by spectroscopic methods and an extended X-ray absorption fine structure study.<sup>22</sup> The formation of a low-valent technetium complex is explained by the stepwise hydrolytic degradation of Haha, which serves as reducing agent and as source of NO in such reactions. This is in accord with previous studies, which describe the decomposition of hydroxamic acids into hydroxylamine and the corresponding carboxylic acids.<sup>23</sup>

Received: January 29, 2014

Published: May 5, 2014

In continuation of our interest in the hitherto almost unexplored fluorine chemistry of technetium with the metal in lower oxidation states, we treated  $K_2[TcF_6]$  with Haha in water, which gave orange-red crystals of the composition  $[Tc(NO)(NH_3)_4F]_4[TcF_6][HF_2]_2$ .<sup>10,11</sup> The reaction, however, takes a couple of days and is hard to control, as can be seen from the presence of hexafluorodotechnetate(IV) as one of the counterions of the product.

In the present Paper, we report a facile synthesis of the technetium(II) complex  $[Tc(NO)F_5]^{2-}$ , which is readily formed from pertechnetate and Haha together with the cation  $[Tc(NO)(NH_3)_4F]^+$ , as well as some of the reactions of the novel nitrosyltechnetium compounds.

## EXPERIMENTAL SECTION

**Materials.** All reagents were reagent grade and used without further purification.  $^{99}Tc$  was purchased as solid ammonium pertechnetate from Oak Ridge National Laboratory (ORNL). The salt was purified by recrystallization from aqueous solutions. For this, the gray-black crystalline solid obtained from ORNL was dissolved in a minimum amount of warm water (60 °C) and filtered through a fine-porous glass frit, leaving behind a very small amount of a black solid ( $TcO_2 \cdot nH_2O$ ). The filtrate was brought to dryness by evaporation of the water, giving large colorless crystals of pure  $(NH_4)TcO_4$ .

**Radiation Precautions.** *Caution!*  $^{99}Tc$  is a long-lived weak  $\beta^-$  emitter ( $E_{max} = 0.292$  MeV). Normal glassware provides adequate protection against the weak  $\beta$  radiation when milligram amounts are used. Secondary X-rays play a significant role only when larger amounts of  $^{99}Tc$  are handled. All manipulations were done in a laboratory approved for the handling of radioactive materials.

**Physical Measurements.** IR spectra were measured with a Shimadzu IR Affinity-1 spectrometer between 400 and 4000  $cm^{-1}$ . Raman spectra were recorded on a RFS 100 instrument (Bruker), and ultraviolet/visible (UV/vis) spectra were taken on a SPECORD 40 instrument (Analytik Jena). The  $^{99}Tc$ ,  $^{19}F$ , and  $^1H$  NMR spectra were recorded on a JEOL-400 MHz nuclear magnetic resonance spectrometer. The electron paramagnetic resonance (EPR) spectra were recorded on an ER 200D-SCR spectrometer with a Bruker B-E25 magnet and an ER 041MR microwave generator. Simulated spectra were obtained by Bruker SIMFONIA based on second-order perturbation theory. Tc values were determined by liquid scintillation counting.<sup>24</sup>

Cyclic voltammetry measurements were performed with a PCI4 (Gamry Instruments) by using a conventional three-electrode cell with working and counter platinum wire electrodes and a Ag/AgCl reference electrode ( $[KCl] = 3$  M). The measurements were carried out in aqueous solutions with a scan rate of 0.1  $V s^{-1}$  at  $T = 293$  K with KF as supporting electrolyte. Potentials were quoted relative to the normal hydrogen electrode.

**X-ray Crystallography.** The intensities for the X-ray determinations were collected on a STOE IPDS 2T instrument with Mo  $K\alpha$  radiation ( $\lambda = 0.71073$  Å) at 200 K. Standard procedures were applied for data reduction and absorption correction. Structure solution and refinement were performed with SHELXS97 and SHELXL97.<sup>6</sup> Hydrogen atom positions were calculated for idealized positions and treated with the "riding model" option of SHELXL.

The obtained single crystals of  $[Tc(NO)(py)_4F](PF_6)$  exhibited twinning by pseudomerohedry.<sup>25</sup> The preliminary description of the structure of  $[Tc(NO)(py)_4F]PF_6$  involves disorder within a lattice of  $C2/c$  symmetry. The structure was solved in the triclinic space group  $P\bar{1}$  by applying the twin law 0 -1 0, -1 0 0, 0 0 -1. More details on data collections and structure calculations are contained in Table 1.

**Computational Details.** All calculations were performed by Gaussian09 C.01.<sup>26</sup> Optimizations and frequency determinations were conducted using the hybrid density functional B3LYP<sup>27-29</sup> together with the basis set 6-311++G\*\* for all atoms excluding Tc,<sup>30</sup> and for technetium the Stuttgart 1997 ECP was used.<sup>31</sup> An exception is the pyridine (py)-containing complex: instead of 6-311++G\*\*, 6-31++G\*\*

is used because of convergence problems in the geometry optimizations. All obtained geometries were identified via the numbers of negative frequencies as minima ( $NImag = 0$ ). Population analysis was performed using natural bond orbital (NBO) and Mulliken as implemented in Gaussian09.<sup>32</sup>

**Syntheses.**  $K_2[Tc(NO)F_5] \cdot H_2O$  and  $[Tc(NO)(NH_3)_4F](PF_6) \cdot 1/2KPF_6 \cdot NH_4TcO_4$  (0.2 mmol, 36 mg) was dissolved in 7 mL of  $HF_{(aq)}$  (48%). Haha (6 mmol, 0.450 g) dissolved in 1 mL of water was added. The color of the solution immediately changed to dark orange-red. The reaction mixture was heated on reflux for 2 h, which resulted in a dark blue solution.  $KPF_6$  (0.5 mmol, 92 mg) in 1 mL of water was added, and the solution was kept at room temperature for crystallization. Two products were obtained. Blue crystals of  $K_2[Tc(NO)F_5] \cdot H_2O$  crystallized first and were separated by filtration. From the remaining mother liquor, orange-red crystals of  $[Tc(NO)(NH_3)_4F](PF_6) \cdot 1/2KPF_6$  were isolated.

$K_2[Tc(NO)F_5] \cdot H_2O$ : Yield 32 mg, 50%. Anal. Calcd for  $F_5H_2K_2NO_2Tc$ : Tc, 30.9; Found: Tc, 30.1%. IR ( $\nu_{max}/cm^{-1}$ ): 3585 br, 1780 s, 1768 sh, 1643 m, 1525 m, 1431 m, 1234 m, 627 sh, 610 s, 567 sh, 529 s, 482 s, 287 sh, 265 s, 212 vw. Raman ( $\nu_{max}/cm^{-1}$ ): 1778 s, 1766 sh, 627 sh, 610 s, 574 s, 527 vw, 534 vw, 501 m, 482 vw, 291 sh, 274 s, 227 s, 218 sh, 137 s, 97 m.

$[Tc(NO)(NH_3)_4F](PF_6) \cdot 1/2 KPF_6$ : Yield 16 mg, 36%. Anal. Calcd for  $F_{10}H_{12}K_{0.5}N_5O_{1.5}Tc$ : Tc, 21.8; Found: Tc, 20.9%. IR ( $\nu_{max}/cm^{-1}$ ): 3367 w, 3303 w, 3202 w, 2958 w, 2640 w, 1677 s, 1626 m, 1532 m, 1291 s, 1268 sh, 997 m, 868 sh, 824 sh, 740 m, 629 m, 553 s. UV/vis: in  $H_2O$ :  $\lambda = 269$  nm ( $\epsilon = 202.0$   $M^{-1} cm^{-1}$ ), 364 nm ( $\epsilon = 36.1$   $M^{-1} cm^{-1}$ ) and 458 nm ( $\epsilon = 45.1$   $M^{-1} cm^{-1}$ ).  $^{99}Tc$  NMR ( $D_2O$ , ppm):  $\delta$  1933 ( $\Delta\nu_{1/2} = 2700$  Hz).  $^{19}F$  NMR ( $D_2O$ , ppm):  $\delta$  -73 (d,  $PF_6^-$ ), -142 (trans Tc-F).

$Rb_2[Tc(NO)F_5] \cdot H_2O$  and  $[Tc(NO)(NH_3)_4F](HF_2) \cdot 1/2RbF$ .  $NH_4TcO_4$  (0.2 mmol, 36 mg) was dissolved in 7 mL of  $HF_{(aq)}$  (48%). Haha (6 mmol, 0.450 g) in 1 mL of water was added. The color of the solution changed to dark orange-red. The reaction mixture was heated on reflux for 2 h.  $RbF$  (0.5 mmol, 52 mg) was added in 1 mL of  $HF_{(aq)}$  (48%), and the resulting solution was kept at room temperature for crystallization. Two products were obtained. Blue crystals of  $Rb_2[Tc(NO)F_5] \cdot H_2O$  crystallized first and were separated by filtration. From the remaining mother solution, orange-red crystals of  $[Tc(NO)(NH_3)_4F](HF_2) \cdot 1/2RbF$  deposited.

$Rb_2[Tc(NO)F_5] \cdot H_2O$ : Yield 41 mg, 50%. Anal. Calcd for  $F_5H_2Rb_2NO_2Tc$ : Tc, 23.9; Found: Tc, 23.1%. IR ( $\nu_{max}/cm^{-1}$ ): 3582 br, 1780 s, 1768 sh, 1648 m, 1432 m, 1194 m, 626 sh, 610 s, 561 sh, 525 s, 505 sh, 480 s, 279 m, 260 s, 208 w. Raman ( $\nu_{max}/cm^{-1}$ ): 1775 s, 1766 sh, 622 s, 568 s, 499 w, 288 s, 267 s, 224 s, 130 s, 112 s, 97 m.

$[Tc(NO)(NH_3)_4F](HF_2) \cdot 1/2 RbF$ : Yield 12.3 mg, 40%. Anal. Calcd for  $F_{3.5}H_{13}N_5ORb_{0.5}Tc$ : Tc, 32.2; Found: Tc, 31.5%. IR ( $\nu_{max}/cm^{-1}$ ): 3578 w, 3322 w, 3194 w, 3089 w, 2878 w, 1782 m, 1653 s, 1620 m, 1485 m, 1417 s, 1298 m, 1270 m, 1211 s, 1066 m, 999 m, 757 s, 734 s, 635 m, 525 s.  $^{99}Tc$  NMR ( $D_2O$ , ppm):  $\delta$  1926 ( $\Delta\nu_{1/2} = 2700$  Hz).  $^{19}F$  NMR ( $D_2O$ , ppm):  $\delta$  -147.9 (s), (Tc-F), -151.1 (s), ( $HF_2^-$ ).

$[Tc(NO)(py)_4F](PF_6)$ . (a)  $K_2[Tc(NO)F_5] \cdot H_2O$  (0.1 mmol, 34 mg) was dissolved in 1 mL of  $HF_{(aq)}$  (48%). Py (2 mL) was added, and the mixture was heated on reflux for 1 h. The volume was reduced to 0.5 mL, and  $KPF_6$  (0.1 mmol, 18.4 mg) was added in 0.3 mL of water. Orange-red crystals of  $[Tc(NO)(py)_4F](PF_6)$  formed upon slow evaporation of the solvent. Yield 36 mg, 60%.

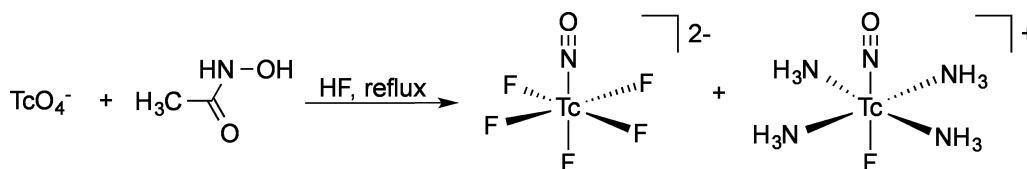
(b)  $NH_4TcO_4$  (0.1 mmol, 34 mg) was dissolved in 2 mL of  $HF$  (48%). Py (6 mL) and Haha (3 mmol, 0.225 g) in 1 mL of water were added, and the mixture was heated for 2 h. The volume was reduced to 0.5 mL, and  $KPF_6$  (0.1 mmol, 18.4 mg) in 0.3 mL of water was added. Orange-red crystals formed upon slow evaporation of the remaining solvent. Yield: 37 mg, 60%.

(c)  $[Tc(NO)(NH_3)_4F]PF_6 \cdot 1/2KPF_6$  (0.03 mmol, 14 mg) was dissolved in 1 mL of  $HF_{(aq)}$  (48%). Py (2 mL) was added, and the mixture was heated on reflux for 1 h. The volume was reduced to 0.5 mL, and orange-red crystals of  $[Tc(NO)(py)_4F](PF_6)$  formed upon slow evaporation of the remaining solvent. Yield 12 mg, 66%.

Anal. Calcd for  $C_{20}H_{20}F_7N_5OPTc$ : Tc, 16.2; Found: Tc, 15.7%. IR ( $\nu_{max}/cm^{-1}$ ): 3115 w, 1699 s, 1604 m, 1566 m, 1487 s, 1448 s, 1363 m,

Table 1. Crystal Data and Refinement Parameters

	$K_2[Tc(NO)F_5] \cdot H_2O$	$Rb_3[Tc(NO)F_5] \cdot H_2O$	$[Tc(NO)(NH_3)_4F](PF_6)_2$	$[Tc(NO)(NH_3)_4F](HF_2)_2$	$[Tc(NO)(NH_3)_4F](SO_4) \cdot H_2O$	$[Tc(NO)(py)_4F]PF_6$	$[Tc(NO)(NH_3)_4(CF_3COO)](CF_3COO) \cdot CF_3COOH$	$[Tc(NO)(NH_3)_4(CF_3COO)](CF_3COO) \cdot EtOH$	$(AsPh_4)[Tc(NO)Cl_4] \cdot EtOH$
formula	$F_5K_2NO_2Tc$	$F_3Rb_2NO_2Tc$	$F_{20}H_{24}KN_{10}O_{21}P_3Tc$	$F_3H_{13}N_5ORb_{10}S_2Tc$	$FH_{12}N_5O_8STc$	$C_{20}H_{20}F_7N_5OPTc$	$C_6H_{13}F_9N_5O_7Tc$	$C_{28}H_{32}AsCl_4NO_3Tc$	
crystal system	orthorhombic	orthorhombic	tetragonal	tetragonal	monoclinic	triclinic	triclinic	monoclinic	
space group	$Cmcm$	$Cmcm$	$P4/m$	$I4/m$	$P2_1/c$	$P\bar{1}$	$P\bar{1}$	$P2_1/n$	
<i>a</i> (Å)	6.203(1)	6.469(1)	12.304(1)	16.454(2)	7.510(1)	9.373(1)	7.133(1)	10.904(1)	
<i>b</i> (Å)	18.654(4)	18.960(3)	12.304(1)	16.454(2)	13.535(1)	9.379(1)	9.323(1)	17.594(1)	
<i>c</i> (Å)	6.301(2)	6.492(1)	8.488(1)	6.938(1)	11.982(1)	14.433(1)	14.198(1)	17.046(1)	
$\alpha$ (deg)	90	90	90	90	90	104.47(1)	99.65(1)	90	
$\beta$ (deg)	90	90	90	90	125.85(1)	104.420(1)	99.64(1)	103.16(1)	
$\gamma$ (deg)	90	90	90	90	90	98.24(1)	98.18(1)	90	
<i>V</i> (Å <sup>3</sup> )	729.1(3)	796.3(2)	1285(2)	1878.4(4)	985.8(2)	1161.8(2)	902.0(2)	3184.3(4)	
<i>Z</i>	4	4	2	8	4	2	2	4	
$\rho_{calc}$ (g·cm <sup>-3</sup> )	2.890	3.420	2.337	2.167	2.205	1.739	1.974	1.555	
$\mu$ (mm <sup>-1</sup> )	3.161	13.997	1.592	4.127	1.706	0.768	0.928	1.848	
reflections collected	886	2951	6114	10947	6372	12 961	10 086	20 156	
reflections unique	384	620	1848	1378	2143	6238	4834	6925	
data/restraints	348/0	564/0	1650/0	1130/0	1839/0	3624/0	4235/0	4202/0	
parameters	39	38	105	64	128	318	268	348	
absorption correction	integration	integration	none	integration	integration	none	none	integration	
max/min transmission	0.877/0.558	0.504/0.078		0.641/0.434	0.908/0.662			0.8231/0.6525	
<i>R</i> 1 [ <i>I</i> > 2 $\sigma$ ( <i>I</i> )]	0.0636	0.0546	0.0400	0.0797	0.0291	0.0647	0.0387	0.0358	
<i>wR</i> 2 [ <i>I</i> > 2 $\sigma$ ( <i>I</i> )]	0.1784	0.1430	0.1043	0.2114	0.0792	0.1290	0.1010	0.0468	
GOF	1.111	1.113	1.079	1.071	1.061	0.865	1.040	0.812	
CSD	CCDC 981 920	CCDC 981 921	CCDC 981 922	CCDC 981 923	CCDC 981 924	CCDC 981 925	CCDC 981 926	CCDC 981 927	

Scheme 1. Reaction of  $\text{TcO}_4^-$  with Acetohydroxamic Acid in HF

1219 m, 1155 m, 1066 m, 1049 m, 877 sh, 840 s, 763 sh, 761 s, 698 s, 635 m, 557 s, 505 m, 464 m. UV/vis in  $\text{CH}_3\text{CN}$ :  $\lambda = 247 \text{ nm}$  ( $\epsilon = 18334 \text{ M}^{-1} \text{ cm}^{-1}$ ),  $360 \text{ nm}$  ( $\epsilon = 16944 \text{ M}^{-1} \text{ cm}^{-1}$ ),  $442 \text{ nm}$  ( $\epsilon = 39.5 \text{ M}^{-1} \text{ cm}^{-1}$ ).  $^1\text{H NMR}$  ( $\text{CD}_3\text{CN}$ , ppm):  $\delta$  8.63 (d), 7.37 (t), 7.80 (t).  $^{13}\text{C NMR}$  ( $\text{CD}_3\text{CN}$ , ppm):  $\delta$  150.8 (d), 138.9 (s), 125.9 (d).  $^{99}\text{Tc NMR}$  ( $\text{CD}_3\text{CN}$ , ppm):  $\delta$  1721 ( $\Delta\nu_{1/2} = 650 \text{ Hz}$ ).  $^{19}\text{F NMR}$  ( $\text{CD}_3\text{CN}$ , ppm):  $\delta$  -73.7 (d,  $\text{PF}_6^-$ ), -171 (trans  $\text{Tc}-\text{F}$ ).

$[\text{Tc}(\text{NO})(\text{NH}_3)_4(\text{OOCF}_3)](\text{OOCF}_3)\cdot\text{CF}_3\text{COOH}$ .  $[\text{Tc}(\text{NO})(\text{NH}_3)_4\text{F}](\text{HF}_2)\cdot 1/2\text{RbF}$  (0.01 mmol, 7 mg) was dissolved in trifluoroacetic acid (0.5 mL), and the solution was left to evaporate slowly at room temperature. Orange crystals of  $[\text{Tc}(\text{NO})(\text{NH}_3)_4(\text{OOCF}_3)](\text{OOCF}_3)\cdot\text{CF}_3\text{COOH}$  were obtained. Yield 10 mg, 90%. Anal. Calcd for  $[\text{Tc}(\text{NO})(\text{NH}_3)_4(\text{OOCF}_3)](\text{OOCF}_3)\cdot\text{CF}_3\text{COOH}$ : Tc, 18.4; Found: Tc, 17.7%. IR ( $\nu_{\text{max}}/\text{cm}^{-1}$ ): 3348 br, 3303 br, 3269 br, 3147 br, 1670 s, 1656 sh, 1439 s, 1421 m, 1290 s, 1180 s, 1139 s, 1115 m, 852 m, 829 s, 799 s, 752 m, 717 s, 614 m, 599 m. Raman ( $\nu_{\text{max}}/\text{cm}^{-1}$ ): 1684 m, 1439 s, 1421 m, 1088 br, 852 m, 834 m, 726 m, 625 s, 598 sh, 500 m, 463 m, 418 m, 404 m, 264 m, 196 s.  $^{99}\text{Tc NMR}$  ( $\text{CD}_3\text{CN}$ , ppm):  $\delta$  2017 ( $\Delta\nu_{1/2} = 3840 \text{ Hz}$ ).  $^{19}\text{F NMR}$  ( $\text{CD}_3\text{CN}$ , ppm):  $\delta$  -76.27 and -76.3 ( $\text{CF}_3$ ).  $^1\text{H NMR}$  ( $\text{CD}_3\text{CN}$ , ppm):  $\delta$  2.54 (s) ( $\text{NH}_3$ ).

$[\text{Tc}(\text{NO})(\text{NH}_3)_4\text{F}](\text{SO}_4)$ .  $[\text{Tc}(\text{NO})(\text{NH}_3)_4\text{F}](\text{PF}_6)\cdot 1/2\text{KPF}_6$  (0.08 mmol, 35 mg) was dissolved in 1.5 mL of  $\text{HF}_{(\text{aq})}$  (48%).  $\text{Ce}(\text{SO}_4)_2\cdot 4\text{H}_2\text{O}$  (0.1 mmol, 40 mg) in 1 mL of warm  $\text{H}_2\text{O}$  was added dropwise. The reaction mixture was kept at  $70^\circ\text{C}$  for 1 h. The color of the solution turned from orange-red to green, and a colorless precipitate formed. After filtration,  $\text{Na}_2\text{SO}_4$  (0.4 mmol, 56 mg) in 1 mL of water was added, and the resulting clear solution was kept for evaporation. Green crystals of  $[\text{Tc}(\text{NO})(\text{NH}_3)_4\text{F}](\text{SO}_4)\cdot\text{H}_2\text{O}$  were obtained. Yield 16 mg, 62%. Anal. Calcd for  $\text{FH}_{14}\text{N}_3\text{O}_6\text{STc}$ : Tc, 29.9; Found: Tc, 29.1%. IR ( $\nu_{\text{max}}/\text{cm}^{-1}$ ): 3315 br, 3230 br, 3156 br, 3070 br, 1816 s, 1641 m, 1591 m, 1430 m, 1334 s, 1067 s, 1029 sh, 959 m, 876 m, 825 s, 794 s, 741 sh, 625 w, 484 w, 468 w, 452 w, 606 s, 556 s. Raman ( $\nu_{\text{max}}/\text{cm}^{-1}$ ): 3170 w, 3233 w, 1807 s, 1660 w, 1615 w, 1550 w, 1369 s, 1342 s, 1333 sh, 1310 m, 1131 m, 1020 w, 994 sh, 957 s, 749 m, 619 s, 530 s, 487 s, 469 m, 442 m, 303 sh, 253 s, 199 sh, 151 m, 117 s, 83 s.

$\text{Na}_2[\text{Tc}(\text{NO})\text{Cl}_5]$ .  $\text{NH}_4\text{TcO}_4$  (0.2 mmol, 36 mg) was dissolved in 7 mL of  $\text{HCl}_{(\text{aq})}$  (37%). Haha (6 mmol, 0.450 g) in 1 mL of water was added. The reaction mixture was heated on reflux for 2 h. The color of the solution changed from dark orange-red to green. Addition of  $\text{NaCl}$  (0.5 mmol, 29 mg) in 1 mL of  $\text{H}_2\text{O}$  resulted in the precipitation of green crystals of  $\text{Na}_2[\text{Tc}(\text{NO})\text{Cl}_5]$ . Yield 35 mg, 50%. Anal. Calcd for  $\text{Cl}_5\text{NNa}_2\text{OTc}$ : Tc, 28.09; Found: Tc, 28.0%. IR ( $\nu_{\text{max}}/\text{cm}^{-1}$ ): 3611 w, 3175 br, 3040 m, 1871 s, 1784 s, 1391 m, 604 s, 571 m.

$(\text{AsPh}_4)[\text{Tc}(\text{NO})\text{Cl}_4(\text{C}_2\text{H}_5\text{OH})]\cdot\text{C}_2\text{H}_5\text{OH}$ .  $\text{NH}_4\text{TcO}_4$  (0.2 mmol, 36 mg) was dissolved in 7 mL of  $\text{HCl}_{(\text{aq})}$  (37%). Haha (6 mmol, 0.450 g) in 1 mL of water was added. The reaction mixture was heated on reflux for 2 h. The color of the solution changed from dark orange-red to green. Addition of  $\text{AsPh}_4\text{Cl}\cdot\text{H}_2\text{O}$  (0.5 mmol, 209 mg) in 1 mL of  $\text{H}_2\text{O}$  resulted in the precipitation of a green solid. Recrystallization from  $\text{EtOH}/\text{CH}_2\text{Cl}_2$  (2:1) gave dark green crystals of  $(\text{AsPh}_4)[\text{Tc}(\text{NO})\text{Cl}_4(\text{C}_2\text{H}_5\text{OH})]\cdot\text{C}_2\text{H}_5\text{OH}$  (89 mg, yield: 60%) and yellow crystals of  $(\text{AsPh}_4)_2[\text{Tc}(\text{NO})\text{Cl}_5]$  (56 mg, yield: 40%). Anal. Calcd for  $\text{C}_{28}\text{H}_{32}\text{AsCl}_4\text{NO}_3\text{Tc}$ : Tc, 13.3; Found: Tc, 13.0%. IR ( $\nu_{\text{max}}/\text{cm}^{-1}$ ): 3485 w, 3150 br, 3056 s, 2961 w, 2922 m, 1783 s, 1759 sh, 1649 m, 1620 m, 1577 s, 1480 s, 1437 s, 1381 m, 1338 m, 1312 m, 1277 m, 1186 s, 1164 m, 1079 s, 1036 s, 995 s, 920 m, 878 s, 842 m, 804 m, 738 s, 685 s, 628 m, 606 w, 581 w.

## RESULTS AND DISCUSSION

Aqueous Haha reacts with  $\text{NH}_4\text{TcO}_4$  in hydrofluoric acid (48%) and forms an orange-red solution, which turned bluish-green

upon heating. The course of the reaction was followed by both  $^{99}\text{Tc}$  NMR and EPR spectroscopy. After heating the reaction mixture in HF, the absence of a pertechnetate signal in the  $^{99}\text{Tc}$  NMR spectrum confirms the complete reduction of the  $\text{Tc}(\text{VII})$  starting material. Simultaneous EPR measurements of the resulting blue reaction mixture indicate the formation of  $[\text{Tc}(\text{NO})\text{F}_5]^{2-}$  as the major product, together with some traces of a second paramagnetic compound (most probably the recently described  $[\text{Tc}(\text{NO})(\text{aha})_2(\text{H}_2\text{O})]^+$ ).<sup>22</sup> Treatment of such solutions with alkali metal fluoride salts  $\text{MF}$  ( $\text{M} = \text{K}, \text{Rb}$ ) or  $\text{KPF}_6$  give blue crystals of  $\text{M}_2[\text{Tc}(\text{NO})\text{F}_5]\cdot\text{H}_2\text{O}$  ( $\text{M} = \text{K}, \text{Rb}$ ) in yields of approximately 50%. Concentration of the remaining pale-blue solution by slow evaporation at room temperature results in a change of the color to orange-yellow. Within a few days, the remaining EPR signal of  $[\text{Tc}(\text{NO})\text{F}_5]^{2-}$  disappeared completely, and a relatively broad  $^{99}\text{Tc}$  NMR signal appeared at about 1930 ppm. Finally, orange-red crystals of a  $\text{Tc}(\text{I})$  ammine complex of the composition  $[\text{Tc}(\text{NO})(\text{NH}_3)_4\text{F}](\text{HF}_2)\cdot 1/2\text{RbF}$  or  $[\text{Tc}(\text{NO})(\text{NH}_3)_4\text{F}](\text{PF}_6)\cdot 1/2\text{KPF}_6$  deposited as a second product from the reaction mixture (Scheme 1).

The source for the nitrosyl and ammine ligands has been explained by the decomposition of Haha in acidic solutions in previous papers.<sup>22,23</sup> A mechanism for the formation of low-valent technetium complexes has been proposed on the basis of kinetic studies and competitive experiments with hydroxylamine. It is highly probable that the reaction does not simply follow the "hydroxylamine reduction of pertechnetate." The coordination of  $\text{aha}^-$  in the initial steps of the reaction cascade seems to be essential, followed by a metal-assisted degradation of the  $\text{aha}^-$  ligands and subsequent reductive nitrosylation. For details see ref 22.

The redox chemistry as well as the ligand-exchange behavior of the obtained nitrosyl complexes of technetium(II) and technetium(I) have been studied. A summary of the attempted reactions and obtained products is given in Scheme 2. The structures of  $\text{K}_2[\text{Tc}(\text{NO})\text{F}_5]$  and  $\text{Rb}_2[\text{Tc}(\text{NO})\text{F}_5]$  were studied by single-crystal diffraction. Both compounds crystallize as monohydrates in the orthorhombic space group  $\text{Cmcm}$ . They are isostructural to other  $\text{M}_2[\text{M}(\text{NO})\text{F}_5]\cdot\text{H}_2\text{O}$  salts ( $\text{M}^1 = \text{K}, \text{Rb}$ ;  $\text{M} = \text{Ru}$ ;  $\text{M}^1 = \text{K}, \text{Rb}, \text{Cs}$ ;  $\text{M} = \text{Os}$ ).<sup>33</sup> Figure 1 shows an ellipsoid plot of the complex anion of the potassium salt together with a visualization of the cation packing. Since the structure of the rubidium compound is virtually identical, no extra figure is shown here. Selected bond lengths and angles of both compounds are given in Table 2.

The technetium atom in  $\text{K}_2[\text{Tc}(\text{NO})\text{F}_5]$  possesses a slightly distorted octahedral coordination environment. It is displaced from the mean least-squares plane of the four equatorial fluorido ligands by 0.182(1) Å. The corresponding value for the rubidium salt is 0.164(1) Å. The  $\text{F1}-\text{Tc}-\text{F2}$  angles are smaller than  $90^\circ$ , and  $\text{N10}-\text{Tc}-\text{F1}$  angles are larger than  $90^\circ$ . These deviations of the angles from  $90^\circ$  can be explained by the formation of the  $\text{Tc}=\text{N}$  double bond. The nitrosyl ligand is linearly coordinated and has a  $\text{N10}-\text{O10}$  bond length of

Scheme 2. Synthesis and Reactions of Nitrosyltechnetium Complexes with Fluorido Ligands

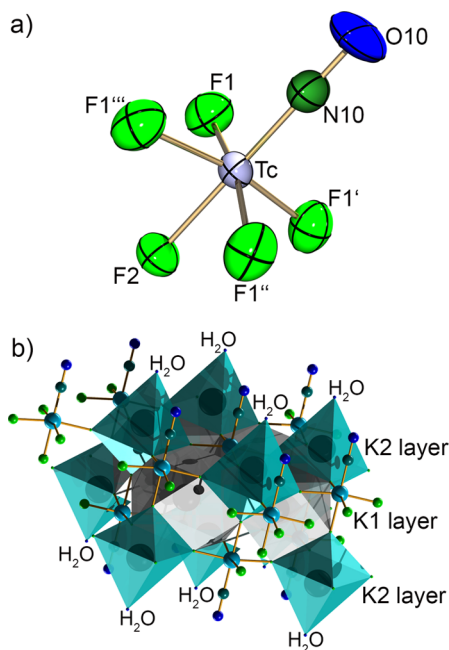
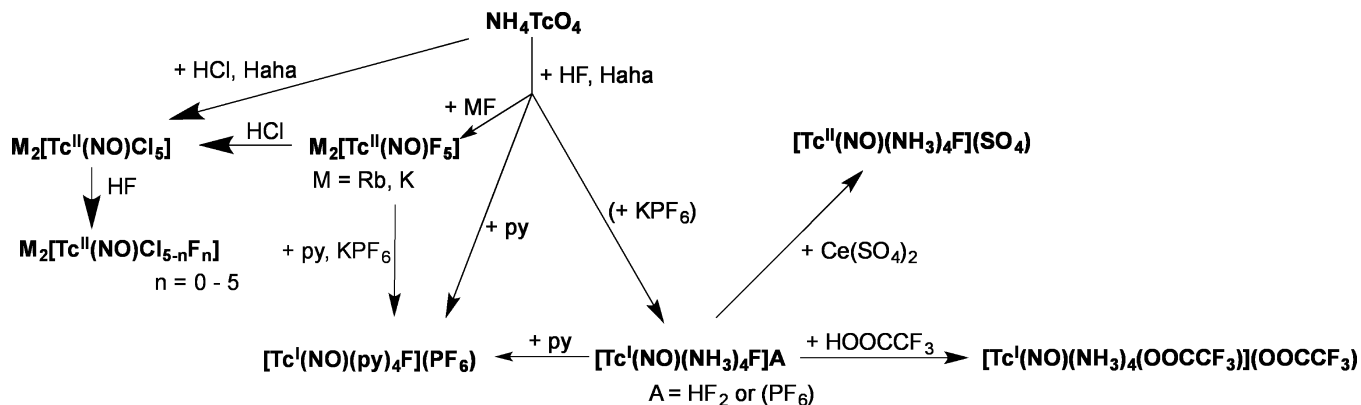


**Figure 1.** (a) Ellipsoid representation of the  $[\text{Tc}(\text{NO})\text{F}_5]^{2-}$  anion in  $\text{K}_2[\text{Tc}(\text{NO})\text{F}_5]$  (symmetry operators: (')  $x, y, 0.5 - z$ , (")  $-x, y, 0.5 - z$ , (""')  $-x, y, z$ ). (b) Coordination polyhedra of the cations (distorted octahedral around K2 and distorted cuboctahedra around K1).<sup>34</sup>

1.15(3) Å, which is typical for nitrosyl ligands of the  $\text{NO}^+$  bonding mode.

The crystallographic results are well-reproduced by density functional theory (DFT) calculations. The appropriate bond lengths and angles obtained from geometry optimization are added to the experimental data in Table 2. Expectedly, the calculated Tc–F and NO bonds are slightly longer than the experimental values, since calculations of gas-phase structures do not consider lattice effects, which definitively play a role in the solid-state structures of the alkaline metal salts. The values of the Tc–N bond and the bond angles inside the molecule, however, are well-reproduced. This includes the N10–Tc–F1 angles of  $93.4^\circ$ , which supports the discussion (below) that this “roof effect” is caused by electron density being located between the technetium and the nitrogen atom.

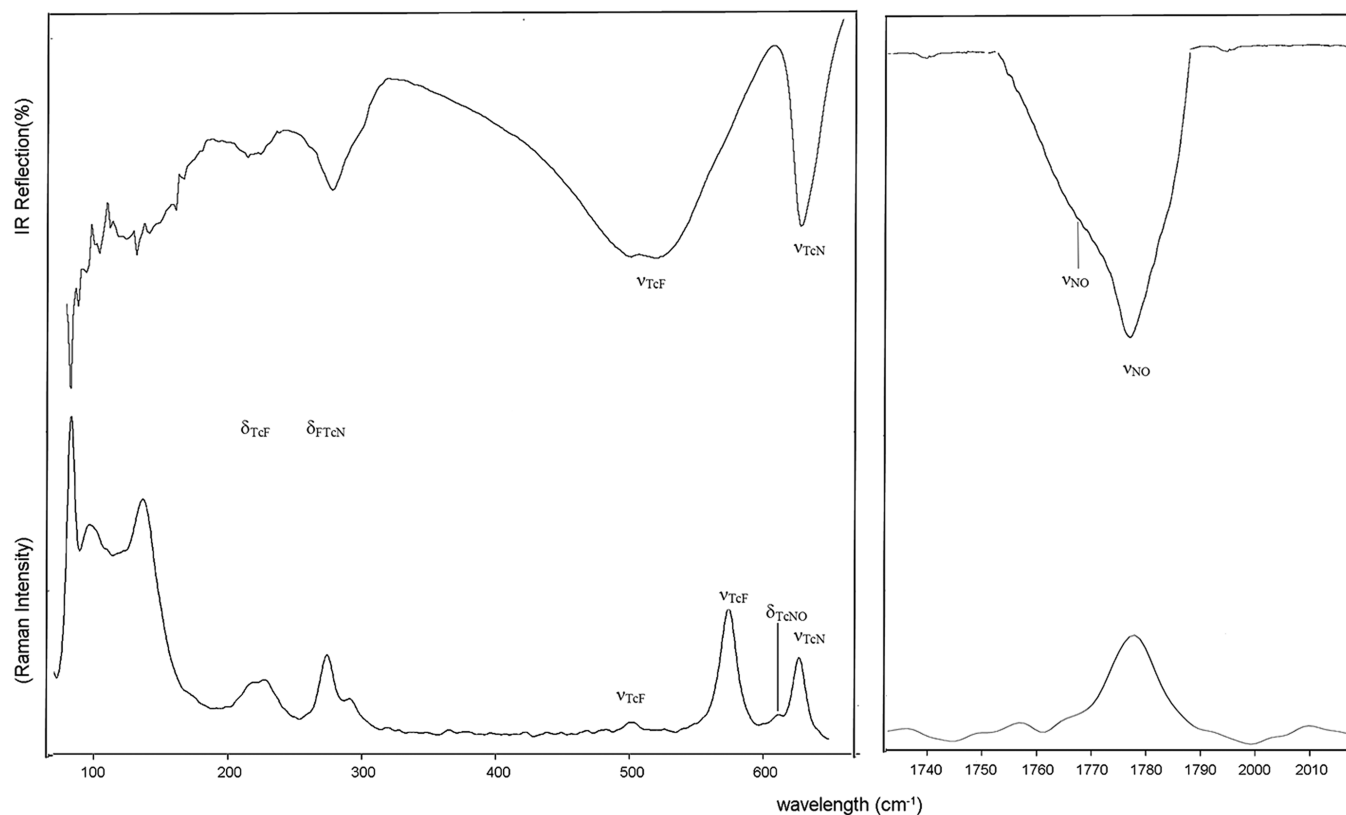
The two potassium cations possess different coordination polyhedra. While K2 is coordinated by each one  $\text{F}^-$  ligand of the adjacent  $[\text{Tc}(\text{NO})\text{F}_5]^{2-}$  units and the solvent water in an elongated octahedral environment, the atom K1 has a

coordination number of 12. Its coordination polyhedron can best be described as a distorted (elongated) cuboctahedron, which shares four of its eight triangular faces with  $\text{F}_3$  triangles of the adjacent  $[\text{Tc}(\text{NO})\text{F}_5]^{2-}$  anions (Figure 1b). The slightly different Tc–F bonds in the anion are consequently the reason for the elongation of the cuboctahedron, which shows rectangular faces instead of squares. Thus, an approximate “8 + 2 + 2 coordination” (2.90 Å to F1, 3.10 Å to F2, and 3.15 Å to F2) is observed for the potassium cations K1 (for details see Figure S1a and Table S1 in the Supporting Information). Finally, an arrangement of the  $\text{K}_2[\text{Tc}(\text{NO})\text{F}_5]$  units in triple layers (see Figure 1 and Supporting Information, Figure S1b) is observed, where two layers of octahedrally coordinated potassium cations K2 embed one layer of the 12-coordinate cations K1. The nitrosyl ligands and the solvent water molecules point to the outer side of these layers, and hydrogen bonds between the water molecules and fluorido ligands connect such triple layers to the observed sandwich structure (see also Supporting Information, Figure S1).

The IR and Raman spectra of  $\text{K}_2[\text{Tc}(\text{NO})\text{F}_5] \cdot \text{H}_2\text{O}$  are shown in Figure 2. The full IR spectrum is reproduced in the Supporting Material as Figure S1–1. Isolated  $[\text{Tc}(\text{NO})\text{F}_5]^{2-}$  anions should have  $C_{4v}$  symmetry, for which 13 vibrational modes ( $\Gamma = 5A_1 + 2B_1 + B_2 + 5E$ ) are expected, and all of them are Raman active. Only  $A_1$  and the E modes are IR active. Since the  $\text{M}_2[\text{Tc}(\text{NO})\text{F}_5] \cdot \text{H}_2\text{O}$  salts ( $M = \text{K}, \text{Rb}$ ) crystallize in the space group  $Cmcm$ , which belongs to the crystal class  $mmm$  ( $D_{2h}$ ), their local symmetry is lowered to  $C_{2v}$ , which can lead to an observable splitting of the E modes (the atoms Tc, F2, N10, and O10 lie on the special position  $m2m$ ). Additionally, in the crystal class  $D_{2h}$ , a weak splitting of the normal modes may occur due to the coupling of the normal modes of the four anions of the unit cell. This is a possible explanation for the observed splitting of the intense N–O stretching vibration in the IR spectrum. The two bands at 627 and 610  $\text{cm}^{-1}$  are assigned to the  $\nu(\text{TcN})$  stretching vibration and  $\delta(\text{TcNO})$  bending vibration by comparison with  $\text{Na}_2[\text{Ru}(\text{NO})\text{F}_5] \cdot \text{H}_2\text{O}$ <sup>35</sup> and  $(\text{CH}_2\text{py}_2)[\text{Ru}(\text{NO})\text{FCl}_4]$ .<sup>36</sup> The band at ca. 520  $\text{cm}^{-1}$  is assigned to the  $\nu_3(A_1)$  mode of  $\nu(\text{TcF})$  vibrations. The vibrational modes between 574 and 482  $\text{cm}^{-1}$  correspond to  $\nu(\text{Tc-F}_{\text{ax}})$  and  $\nu(\text{Tc-F}_{\text{eq}})$  bonds. The observed vibrational modes between 265 and 97  $\text{cm}^{-1}$  correspond to bending modes. The assignment of the bands has been done with the help of DFT calculations, which well reproduce the absorption patterns of the vibrational spectra. The individual frequencies, however, are calculated systematically at too low energies and have to be treated with scaling factors of 1.04 for the N=O

**Table 2.** Selected Bond Lengths (Å) and Angles (deg) in  $K_2[Tc(NO)F_5]$  and  $Rb_2[Tc(NO)F_5]$  Obtained from X-ray Diffraction and DFT Calculations

	$K_2[Tc(NO)F_5]$	$Rb_2[Tc(NO)F_5]$	$[Tc(NO)F_5]^{2-}$ DFT
Tc–N10	1.74(1)	1.78(1)	1.746
N10–O10	1.15(3)	1.10(2)	1.200
Tc–F1	1.937(8)	1.961(4)	2.019
Tc–F2	1.96(1)	2.00(1)	2.008
Tc–N10–O10	180	180	180
N10–Tc–F1	95.4(2)	94.8(1)	93.4

**Figure 2.** IR and Raman spectra of  $K_2[Tc(NO)F_5] \cdot H_2O$ .**Table 3.** EPR Parameters of Tc(II) Nitrosyl Complexes

compound	$g_{\parallel}^a$	$g_{\perp}^a$	$A_{\parallel}^a$	$A_{\perp}^a$	$g_0^a$	$a_0^{Tc\alpha}$	ref.
$[Tc(NO)F_5]^{2-b}$	1.883	2.019	332	144	1.9736	203.5	this study
$[Tc(NO)Cl_5]^{2-}$	1.992	2.052	261.2	104.0			this study
$[Tc(NO)(NH_3)_4F]^{2+}$	1.959	2.051	271.2	112.4			this study
$[Tc(NO)(NH_3)_5(H_2O)]^{3+}$	1.861	2.114	296.6	108.8	2.026	165.4	40
$[Tc(NO)Cl_4]^{-}$	1.985	2.037	259.8	111.0	2.029	157.6	40
$[Tc(NO)Br_4]^{-}$	2.105	2.081	216.5	89.3	2.089	132.0	41
$[Tc(NO)I_4]^{-}$	2.262	2.144	155.0	73	2.171	103.0	42
$[Tc(NO)(NCS)_5]^{2-}$	1.936	2.042	240.3	99.5	2.013	143.3	43

<sup>a</sup>Coupling constants in  $10^{-4} \text{ cm}^{-1}$ . <sup>b</sup> $a_X^E = a_Y^E = 50 \times 10^{-4} \text{ cm}^{-1}$ ;  $a_Z^E = 2 \times 10^{-4} \text{ cm}^{-1}$ .  $\Delta g = \pm 0.001$ ,  $\Delta A = \pm 1 \times 10^{-4} \text{ cm}^{-1}$ . The  $g$  and  $A$  values were obtained by computer simulation (Bruker SIMFONIA) based on second-order perturbation theory.

stretch and 1.08 for the Tc–N/F bands, respectively, to reproduce the experimental spectra.<sup>37</sup> Such a procedure is not unusual and has also been applied for nitrosyl complexes before.<sup>38</sup> The individual scaling factors depend on the vibrational mode and the basis sets used for the calculations.<sup>37</sup>

The  $d^5$  low-spin configuration ( $S = 1/2$ ) of  $M_2[Tc(NO)F_5] \cdot H_2O$  ( $M = K, Rb$ ) allows the examination of EPR spectra of the complex at ambient conditions. Liquid and frozen-solution EPR

spectra are given in Figure 3. Ten hyperfine lines are resolved due to the interaction of the unpaired electron with the nuclear spin of  $^{99}\text{Tc}$  ( $I = 9/2$ ). The frozen-solution spectrum reflects axial symmetry and can be adequately treated with a spin Hamiltonian as used for other nitrosyl- and thionitrosyltechnetium(II) complexes.<sup>39</sup> The corresponding EPR parameters are compared to the quantities obtained for other  $[Tc(NO)X_{4/5}]^{-/2-}$  complexes ( $X = \text{halide or pseudohalide}$ ) in Table 3. In the perpendicular part

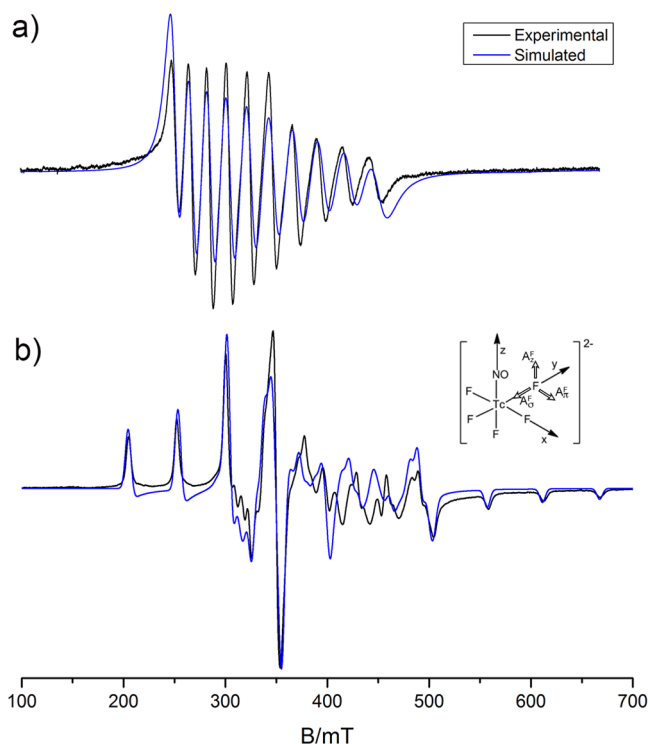


**Figure 3.** X-Band EPR spectra of  $K_2[Tc(NO)F_5] \cdot H_2O$  in HF. (a) At room temperature. (b)  $T = 77K$ .

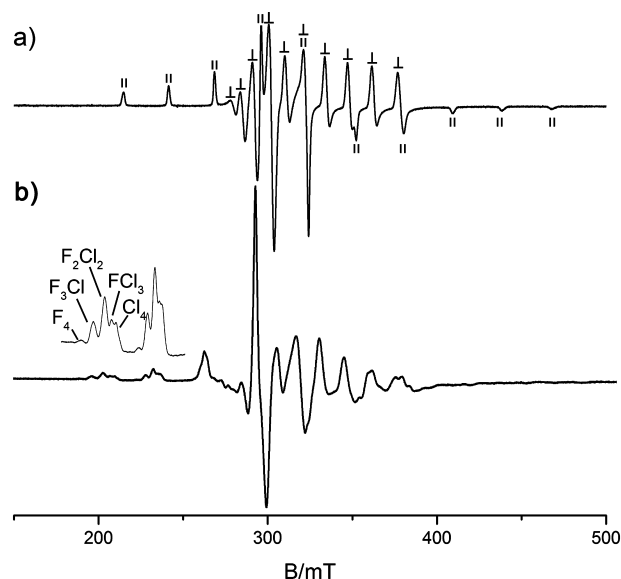
of the spectrum an additional splitting of  $50 \times 10^{-4} \text{ cm}^{-1}$  is observed due to the interaction of the unpaired electron with the equatorial ( $x, y$ ) fluoro ligands ( $^{19}\text{F}$ , nuclear spin  $I = 1/2$ ). The directions of the principal axes of the  $^{19}\text{F}$  ligand hyperfine structure (hfs) tensors in the molecular frames commonly used for  $d^1$  systems are illustrated in Figure 3b. The ligand hfs observed in the perpendicular part of the spectrum does not necessarily correspond to a principal value of the  $^{19}\text{F}$  hfs tensor. There is no direct experimental evidence for the presence of the fifth fluoro ligand coordinated trans to the nitrosyl group. Note that the absence of superhyperfine splitting due to the trans fluoride is not unusual. The same is observed in the cases of  $[MoOF_5]^{2-}$ ,  $[NbOF_5]^{2-}$ , and  $[ReOF_5]^{2-}$ , where the coordination of trans fluoride is well-established.<sup>44–46</sup> Line width considerations limit the component of the superhyperfine interactions parallel to the Tc–NO direction to less than  $2 \times 10^{-4} \text{ cm}^{-1}$ .

Upon dissolution of  $K_2[Tc(NO)F_5]$  in  $H_2O$ , the resulting solution is EPR-silent. Addition of HF (48%) to this aqueous solution, however, reconstitutes the EPR signal of the fluoro complex. This implies that in aqueous solution a species with Tc–Tc interactions is formed. Similar results have been reported for nitridotechnetium(VI) compounds, where treatment of  $Cs_2[TcNCl_5]$  or  $(NBu_4)[TcNCl_4]$  with water gives  $[TcNCl_5]_2(\mu-O)_2^{2-}$ , a bis( $\mu$ -oxido)technetium(VI) compound,<sup>47,48</sup> which also can be reconverted into the mononuclear  $[TcNCl_5]^{2-}$  upon dissolution in concentrated HCl. All attempts to isolate the assumed  $[Tc(NO)F_5]_2(\mu-O)_2^{2-}$  with large cations such as  $NBu_4^+$  or  $AsPh_4^+$  from aqueous solution failed up to now, while the blue crystals of  $K_2[Tc(NO)F_5] \cdot H_2O$  were reformed after complete evaporation of the water.

Heating  $K_2[Tc(NO)F_5]$  in HCl (35%) results in the formation of a greenish-yellow solution, which expectedly contains  $[Tc(NO)Cl_4]^-$  or  $[Tc(NO)Cl_5]^{2-}$  anions as the sole paramagnetic species, as confirmed by EPR spectroscopy.

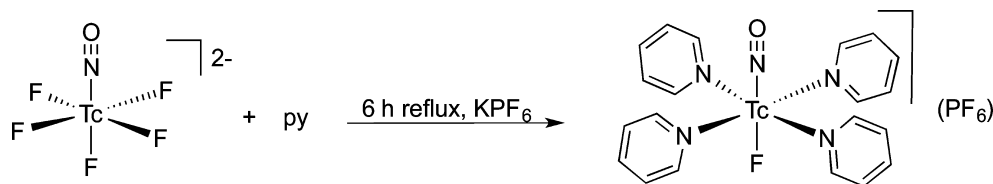
Addition of  $(AsPh_4)Cl$  to such solutions results in the precipitation of a yellow solid. Recrystallization from  $CH_2Cl_2/EtOH$  gave green crystals of  $(AsPh_4)[Tc(NO)Cl_4(EtOH)] \cdot EtOH$ , which were isolated and studied spectroscopically as well as by X-ray diffraction. The structure of the complex anion is very similar to that of the previously published  $(NBu_4)[Tc(NO)Cl_4(MeOH)]$ , which was prepared from reactions of pertechnetate with hydroxylamine hydrochloride.<sup>14</sup> An ellipsoid representation is depicted in Supporting Information, Figure S2. The corresponding bond lengths and angles are summarized in Supporting Information, Table S2. The  $\nu_{NO}$  stretch appears at  $1783 \text{ cm}^{-1}$  in the IR spectrum of the chlorido compound. This value fits well with the reported vibrations found for other  $[Tc(NO)X_{4/5}]^{-/2-}$  complexes.<sup>13,14,40–42</sup> It should be mentioned that  $(AsPh_4)[Tc(NO)Cl_4(EtOH)]$  or the related sodium or tetraethylammonium salts of  $[Tc(NO)Cl_5]^{2-}$  can also be prepared directly from pertechnetate and Haha in HCl following a protocol as described for the synthesis of the  $[Tc(NO)F_5]^{2-}$  salts. However, the formation of significant amount of  $[Tc(NO)Cl_5]^{2-}$  and traces of  $[TcCl_6]^{2-}$  as side products, which are hard to remove, makes such procedures less favorable for the synthesis of a defined nitrosyl chlorido compound. This is in contrast to the synthesis of the fluoro compounds, where only the cationic technetium(I) complex  $[Tc(NO)(NH_3)_4F]^+$ , which can easily be separated from the Tc(II) compound, is formed as a second product.

The frozen-solution EPR spectrum of  $Na_2[Tc(NO)Cl_5]$  is shown in Figure 4a. Ten hyperfine lines are resolved in the



**Figure 4.** Frozen-solution X-Band EPR spectra of (a)  $Na_2[Tc(NO)Cl_5]$  in HCl, with assignment of parallel and perpendicular part lines, and (b) a reaction mixture of  $Na_2[Tc(NO)Cl_5]$  after 6 h of refluxing in aqueous HF (40%). Recording temperature: 77 K.

parallel as well as perpendicular part of the spectrum. The corresponding EPR parameters are given in Table 3. Unlike the reaction of  $K_2[Tc(NO)F_5]$  with HCl, where a rapid ligand exchange  $F^-$  versus  $Cl^-$  proceeds with the corresponding chlorido complex as the sole product, the reaction of  $Na_2[Tc(NO)Cl_5]$  in aqueous HF is slow even at elevated temperatures. At room temperature, almost no reaction could be detected spectroscopically by EPR. Prolonged heating, however, causes a stepwise ligand exchange of the chlorido ligands and the formation of technetium(II) nitrosyl complexes

Scheme 3. Synthesis of  $[\text{Tc}(\text{NO})(\text{py})_4\text{F}](\text{PF}_6)$ 

with a mixed equatorial  $\text{Cl}^-/\text{F}^-$  coordination sphere, which is clearly shown by the signals of the corresponding  $[\text{Tc}(\text{NO})\text{Cl}_n\text{F}_{4-n}(\text{X})]^{-/2-}$  complexes ( $\text{X} = \text{halide}$  or solvent) in the low-field part of the spectra. Figure 4b shows a typical spectrum, in which the parallel part lines of the mixed-ligand species are well-resolved. The perpendicular part lines cannot be assigned individually due to too many line overlappings. As shown earlier for  $[\text{Tc}(\text{NO})\text{Cl}_n\text{Br}_{4-n}]^-$  complexes, the EPR parameters  $g_{\parallel}$  and  $A_{\parallel}$  of the mixed-ligand species show an almost linear dependence on the spin-orbit coupling constants of the (equatorial) donor atoms (cf. Supporting Information, Figure S3 and Table S3).<sup>49,50</sup> This allows the assignment of reactive intermediates by the so-called “additivity rules” on the basis of the quantities of the parent compounds.

A reaction of  $\text{K}_2[\text{Tc}(\text{NO})\text{F}_5]$  with neat boiling pyridine (py) gives a clear solution from which orange-red crystals of  $[\text{Tc}(\text{NO})(\text{py})_4\text{F}](\text{PF}_6)$  precipitated after addition of  $\text{KPF}_6$  and slow evaporation of the mixture (Scheme 3). The complete replacement of the equatorial coordination sphere of technetium by py ligands is without precedent for nitrosyltechnetium complexes. Previous reactions starting from  $(\text{NBu}_4)[\text{Tc}(\text{NO})\text{Cl}_4]$  or  $[\text{Tc}(\text{NO})\text{Cl}_2(\text{PPh}_3)_2(\text{NCCH}_3)]$  with pyridines resulted in the formation of neutral  $[\text{Tc}(\text{NO})\text{Cl}_2(\text{py})_3]$  or mixed phosphine/py complexes.<sup>51</sup>

$[\text{Tc}(\text{NO})(\text{py})_4\text{F}]\text{PF}_6$  is soluble in common organic solvents and also in aqueous hydrofluoric acid. The IR spectrum of the compound shows the  $\text{N}\equiv\text{O}$  stretch at  $1699\text{ cm}^{-1}$ . This value is somewhat higher than those of other Tc(I) complexes, but it is significantly lower than those of the Tc(II) complexes of the present study ( $[\text{Tc}(\text{NO})\text{F}_5]^{2-}$  ( $\sim 1780\text{ cm}^{-1}$ ) and  $[\text{Tc}(\text{NO})(\text{NH}_3)_4\text{F}](\text{SO}_4)$  ( $1830\text{ cm}^{-1}$ )). Bands at  $635$  and  $505\text{ cm}^{-1}$  are assigned to the  $\delta(\text{Tc}-\text{N}-\text{O})$  and  $\nu(\text{Tc}-\text{F})$  vibrations. The  $^{99}\text{Tc}$  NMR signal of the diamagnetic  $[\text{Tc}(\text{NO})(\text{py})_4\text{F}]^+$  cation can be found at  $1721\text{ ppm}$  ( $\Delta\nu_{1/2} = 650\text{ Hz}$ ). This value is outside the range, where chemical shifts of Tc(I) complexes are commonly observed ( $-400$  to  $-3350\text{ ppm}$ ),<sup>12,52,53</sup> but it is in accord with the signal position for  $[\text{Tc}(\text{NO})(\text{NH}_3)_4\text{F}]^+$  ( $\sim 1930\text{ ppm}$ , vide infra). The observed upfield shift of the py complex compared to the ammine complex might be due to the considerably higher degree of back-donation from the metal to the nitrosyl as well as to the pyridine ligands. To prove this, we compare the atomic charges for the two Tc(I) cations  $[\text{Tc}(\text{NO})(\text{py})_4\text{F}]^+$  and  $[\text{Tc}(\text{NO})(\text{NH}_3)_4\text{F}]^+$ . The natural NBO charges for both Tc centers reveal in the pyridine case a value of  $+0.33$  and in the ammine case a value of  $+0.24$ . This is a good hint for enhanced backbonding to py that is not possible with the ammine ligands, because a more positive charge means the electron density is distributed to a higher degree to the ligands, especially when the charges at the F and the NO ligand only change marginally (see Table S8 of the Supporting Information).

The  $^{19}\text{F}$  NMR spectrum of  $[\text{Tc}(\text{NO})(\text{py})_4\text{F}]^+$  shows a resonance at  $-171\text{ ppm}$ , which can be assigned to the fluoro ligand in the axial position. The molecular structure of the  $[\text{Tc}(\text{NO})(\text{py})_4\text{F}]^+$  cation is shown in Figure 5. It shows a

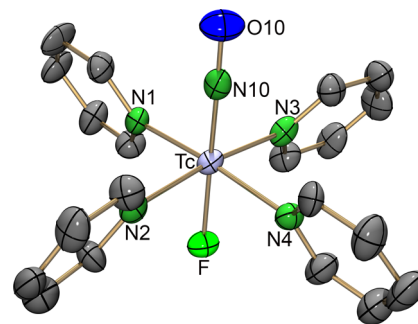


Figure 5. Ellipsoid representation of the complex cation of  $[\text{Tc}(\text{NO})\text{py}_4\text{F}](\text{PF}_6)$ .<sup>54</sup> Hydrogen atoms have been omitted for clarity.

distorted octahedral coordination geometry with four py ligands in equatorial positions. Selected bond lengths and angles are given in Table 4, taken both from crystal structure data and DFT calculations. The  $\text{Tc}-\text{N}10-\text{O}10$  angle of  $177.3(7)^\circ$  is strong evidence for the presence of a  $\text{NO}^+$  moiety. A remarkable feature of the structure is the relatively short  $\text{Tc}-\text{F}$  bond of  $1.954(4)\text{ \AA}$  trans to the nitrosyl ligand. The average  $\text{Tc}-\text{N}_{\text{pyridine}}$  bond length is  $2.145\text{ \AA}$  and, thus, is similar to the values in  $[\text{Tc}(\text{NO})\text{Cl}_2(\text{py})_3]$ .<sup>51</sup> The technetium atom of the  $[\text{Tc}(\text{NO})(\text{py})_4\text{F}]^+$  cation is displaced from the mean least-squares plane of the four py nitrogen atoms by  $0.117(1)\text{ \AA}$  toward the nitrogen atom of the nitrosyl ligand. The py rings give a propeller-like structure around the  $\text{F}-\text{Tc}-\text{NO}$  rotation axis. The dihedral angles between the  $\text{N}_4$  plane and the py rings range from  $63.9(3)$  to  $66.5(3)^\circ$ , with an average value of  $65.4^\circ$ . A similar structure was also found for  $[\text{Ru}(\text{NO})(\text{py})_4\text{Cl}](\text{PF}_6)_2$ .<sup>55</sup>

The cationic ammine complex  $[\text{Tc}(\text{NO})(\text{NH}_3)_4\text{F}]^+$  is the second product that can be isolated from the reaction between pertechnetate and Haha in HF. It crystallizes as the  $\text{HF}_2^-$  or  $\text{PF}_6^-$  salt, depending on the conditions applied and counterions added. The molecular structures of the complex cations are very similar to that of the oxidation product  $[\text{Tc}(\text{NO})(\text{NH}_3)_4\text{F}]^{2+}$ , which will be discussed vide infra. That is why no extra Figures are shown here. Selected bond lengths and angles are summarized in Table 5. The solid-state structures of such salts are characterized by a large number of hydrogen bonds. Figure 6 illustrates the situation in  $[\text{Tc}(\text{NO})(\text{NH}_3)_4\text{F}](\text{HF}_2)\cdot 1/2\text{RbF}$ , and the corresponding H-bonding network in the  $\text{PF}_6^-$  salt is shown in Supporting Information, Figure S5. A summary of the related bond lengths and angles is also given in the Supporting Information (Tables S4 and S5).

The IR spectra of the ammine complexes show the  $\text{N}=\text{O}$  vibrations around  $1650\text{ cm}^{-1}$ . These vibration values are close to the value observed for  $[\text{Tc}(\text{NO})(\text{NH}_3)_4(\text{H}_2\text{O})]\text{Cl}_2$  ( $1680\text{ cm}^{-1}$ ), but they have lower frequencies than those observed for the Tc(II) complexes  $[\text{Tc}(\text{NO})(\text{NH}_3)_4\text{F}](\text{SO}_4)$  ( $1816\text{ cm}^{-1}$ , vide infra) and  $[\text{Tc}(\text{NO})(\text{NH}_3)_4(\text{H}_2\text{O})]\text{Cl}_3$  ( $1830\text{ cm}^{-1}$ ).<sup>56</sup> This reflects a considerable back-donation from the metal ion to the NO ligand in the technetium(I) compounds.



Table 4. Selected Bond Lengths (Å) and Angles (deg) in  $[\text{Tc}(\text{NO})(\text{py})_4\text{F}]\text{PF}_6$ 

	exp.	DFT		exp.	DFT
Tc–N10	1.730(7)	1.741	Tc–N2	2.138(9)	2.185
N10–O10	1.209(8)	1.192	Tc–N3	2.150(9)	2.185
Tc–N1	2.141(8)	2.185	Tc–N4	2.157(8)	2.185
Tc1–F	1.954(4)	2.001			
Tc–N10–O10	177.3(7)	180.0	N10–Tc–N3	93.2(3)	94.0
N10–Tc–F	179.5(4)	180.0	N10–Tc–N3	93.3(4)	94.0
N10–Tc–N2	92.2(4)	94.0	N10–Tc–N4	93.7(3)	94.0

Table 5. Selected Bond Lengths (Å) and Angles (deg) in  $[\text{Tc}(\text{NO})(\text{NH}_3)_4\text{F}]^{+/2+}$  Complexes

	$[\text{Tc}(\text{NO})(\text{NH}_3)_4\text{F}](\text{HF}_2) \cdot 1/2\text{RbF}^a$	$[\text{Tc}(\text{NO})(\text{NH}_3)_4\text{F}](\text{PF}_6) \cdot 1/2\text{K}(\text{PF}_6)^a$	$[\text{Tc}(\text{NO})(\text{NH}_3)_4\text{F}]^{+/2+}$ DFT	$[\text{Tc}(\text{NO})(\text{NH}_3)_4\text{F}](\text{SO}_4)^a$	$[\text{Tc}(\text{NO})(\text{NH}_3)_4\text{F}]^{2+/2+}$ DFT
Tc–N <sub>NO</sub>	1.719(4)	1.715(9)	1.754	1.742(3)	1.800
N–O	1.208(5)	1.20(1)	1.173	1.158(4)	1.141
Tc–N <sub>NH3</sub>	2.169(3), 2.156(3)	2.163(6), 2.166(7)	2.213	2.118(3), 2.121(3) 2.124(3), 2.145(3)	2.200
Tc–F	2.036(3)	2.050(6)	2.017	1.981(2)	1.965
Tc–N–O	179.1(4)	179.7(9)	180	178.6(3)	180
N <sub>NO</sub> –Tc–N	94.2(1), 95.3(1)	93.9(3), 94.4(3)	97.5	93.3(1), 93.6(1), 95.2(1), 95.5(1)	97.1
N <sub>NO</sub> –Tc–F	179.9(2)	178.9(3)		179.8(2)	

<sup>a</sup>For a depiction of the complex cation see Figure 8.

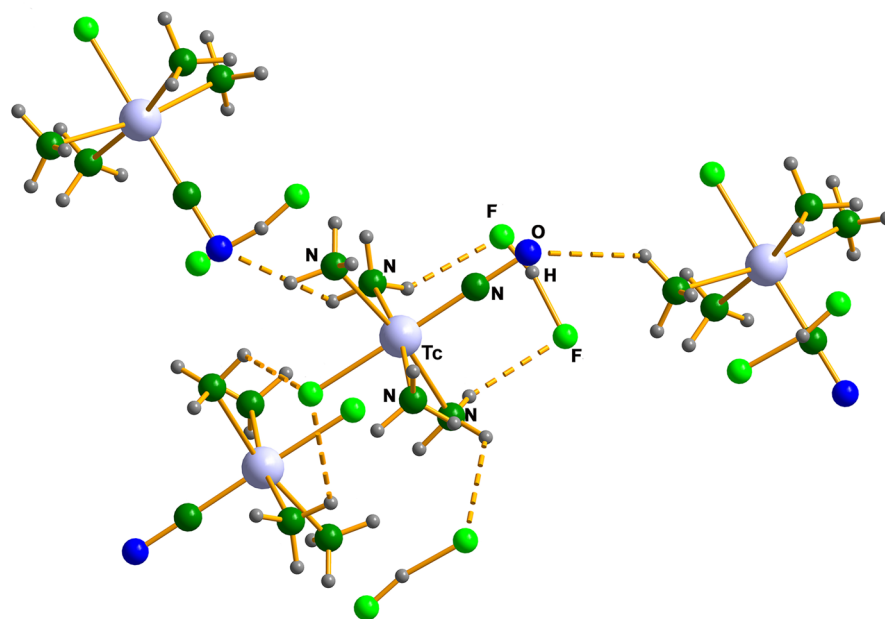


Figure 6. Network of hydrogen bonds in  $[\text{Tc}(\text{NO})(\text{NH}_3)_4\text{F}](\text{HF}_2) \cdot 1/2\text{RbF}$ .<sup>34</sup> For the corresponding bond lengths and angles see Supporting Information, Table S4.

The cocrystallized  $(\text{HF}_2^-)$  anion in  $[\text{Tc}(\text{NO})(\text{NH}_3)_4\text{F}](\text{HF}_2) \cdot 1/2\text{RbF}$  shows a resonance at around  $1250\text{ cm}^{-1}$  ( $\nu_2(E)$ ), the assignment of which was done according to the spectrum of  $\text{NaHF}_2$ .<sup>57</sup>

The formation of the technetium(I) complex  $[\text{Tc}(\text{NO})(\text{NH}_3)_4\text{F}]^+$  is not trivial and self-explanatory, and the mechanism of its formation is not yet clear. On the one hand, the decomposition of hydroxamic acids in acidic media is well-documented, and the formation of hydroxylamine during such reactions is proven.<sup>23</sup> Hydroxylamine has been frequently used as a source for nitrosyl ligands also in the chemistry of technetium, where pertechnetate, oxido complexes, or halo-

genido complexes were converted into nitrosyls by reaction with  $\text{NH}_2\text{OH} \cdot \text{HCl}$ .<sup>14,15,19,40,56,58–60</sup> On the other hand, a carefully done mechanistic study of the reaction of pertechnetate with Haha strongly suggests that the formation of low-valent technetium nitrosyls does not follow a simple “hydroxylamine approach” but that the nitrosylation proceeds on lower-valent technetium species.<sup>22</sup> This is in agreement with our findings, that (i) we did not succeed with the synthesis of the fluoro complexes of this report by other nitrosylation reactions, for example, with hydroxylamine or NO gas, (ii) reactions of prereduced technetium species such as  $[\text{TcF}_6]^{2-}$  with Haha are very slow,<sup>11</sup> and (iii) the formation of the

amminotechnetium(I) complex  $[\text{Tc}(\text{NO})(\text{NH}_3)_4\text{F}]^+$  proceeds in a second, slow reaction from a not-yet characterized low-valent Tc complex (most probably containing  $\text{aha}^-$  ligands as a source for  $\text{NH}_3$ ). It should be mentioned here that we did not observe any evidence for remaining  $\text{TcO}_4^-$  or for  $[\text{Tc}(\text{NO})(\text{NH}_3)_4\text{F}]^+$  in the reaction mixture from which the  $[\text{Tc}(\text{NO})\text{F}_5]^{2-}$  salts precipitate. The signal of the Tc(I) complex only appears after a prolonged reaction time, which strongly indicates that the formation of the ammine ligands originates from an intermediate with nitrogen-containing ligands and is a metal-driven or metal-controlled process. The simultaneous formation of NO and ammine ligands in such acidic media like 40% aqueous HF is hitherto not surely established. During the synthesis of  $[\text{Tc}(\text{NO})(\text{NH}_3)_4(\text{H}_2\text{O})]\text{Cl}_2$ , aqueous ammonia has been added.<sup>15</sup> This compound, frequently also called “Eakins’ pink complex,” was the subject of several careful studies and re-evaluations before its real nature as an ammine complex was established. But it should be mentioned that the typical pink color of the complex is reported to appear before the  $\text{NH}_3$  addition,<sup>15</sup> and a similar reaction with 1,10-phenanthroline gives an ammine complex without the addition of ammonia.<sup>60</sup>

$[\text{Tc}(\text{NO})(\text{NH}_3)_4\text{F}](\text{PF}_6)$  can readily be oxidized to the corresponding technetium(II) complex. The cyclic voltammetry measurement of the compound was undertaken in water under an argon atmosphere. The complex shows a reversible oxidation at 0.652 V ( $\Delta E_p = 107$  mV), corresponding to the expected one-electron transfer process (Figure 7). This value is

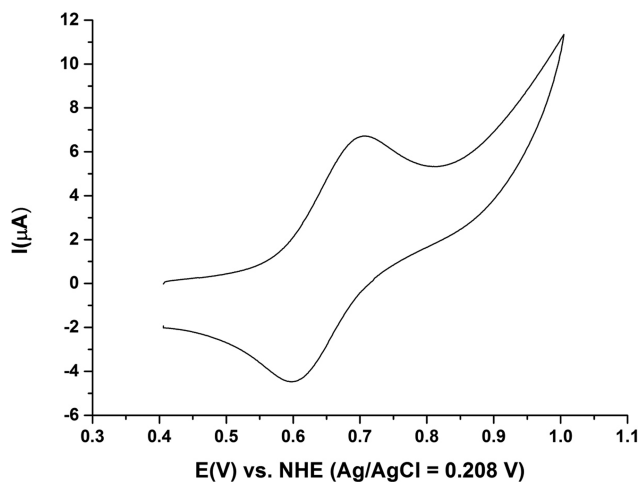


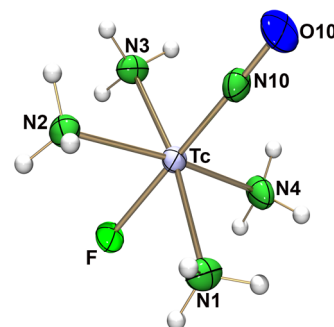
**Figure 7.** Cyclic voltammogram of  $[\text{Tc}(\text{NO})(\text{NH}_3)_4\text{F}](\text{PF}_6)$  in 0.1 M  $\text{KF}/\text{H}_2\text{O}$  at a scan rate of  $100 \text{ mV s}^{-1}$ .

lower than the potential, which was measured earlier for the corresponding aqua complex (0.8 V).<sup>56</sup> But we should keep in mind that the latter value was measured in trifluoromethanesulfonic acid.

The oxidation of the technetium(I) complex can also be performed chemically. Addition of  $\text{Ce}(\text{SO}_4)_2$  to an aqueous solution of  $[\text{Tc}(\text{NO})(\text{NH}_3)_4\text{F}](\text{PF}_6)$  results in a color change, and the resulting green solution shows an intense EPR spectrum (see Supporting Information, Figure S6) with a typical axially symmetric pattern as has been described before. Hyperfine couplings due to  $^{99}\text{Tc}$  are well resolved in the parallel and perpendicular parts, but no other splittings due to the ligand nuclei. This is in accord with the expected “ $d_{xy}$  character” of the MO of the unpaired electron. The corresponding EPR parameters are

compared to the values of other nitrosyltechnetium(II) complexes in Table 3.

Green single crystals of  $[\text{Tc}(\text{NO})(\text{NH}_3)_4\text{F}](\text{SO}_4)\cdot\text{H}_2\text{O}$  are obtained from an aqueous solution of the oxidation mixture after addition of  $\text{Na}_2\text{SO}_4$ . An ellipsoid plot of the complex cation is shown in Figure 8. Relevant bond lengths and angles

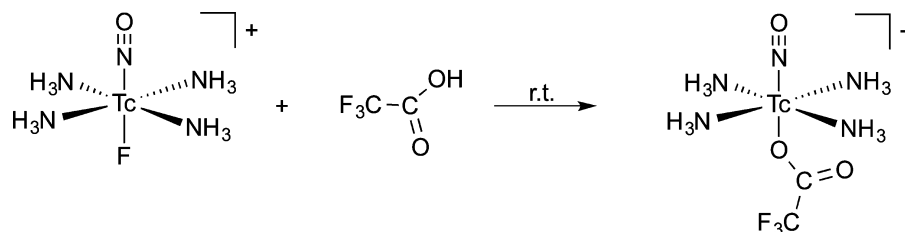


**Figure 8.** Ellipsoid plot of the complex cation of  $[\text{Tc}(\text{NO})(\text{NH}_3)_4\text{F}](\text{SO}_4)$ .<sup>34</sup>

are compared to the values of the corresponding Tc(I) ion in Table 5. The Tc–NO bond length of  $1.742(3)$  Å is slightly longer, and the N–O bond is shorter than the corresponding value in the Tc(I) compounds. This reflects the lower degree of back-donation in the Tc(II) compound, which was already stated on the basis of the IR data. The four ammine ligands are in the equatorial plane, and fluorine is coordinated trans to the nitrosyl ligand. The Tc–N–O angle is  $178.6(3)^\circ$ , and all  $\text{N}_{\text{nitrosyl}}\text{--Tc--NH}_3$  angles are larger than  $90^\circ$ . This is due to the bulk of the Tc–NO multiple bond. The technetium atoms of the  $[\text{Tc}(\text{NO})(\text{NH}_3)_4\text{F}]^{2+}$  cations are displaced from the mean least-squares plane of the four  $\text{NH}_3$  ligands by  $0.164(1)$  Å.

The structural and spectroscopic features of the Tc(I) and Tc(II) ammine complexes are well-reproduced by the DFT calculations performed. A comparison of significant bond lengths and angles is given in Table 5. It is remarkable that all structural changes, which appear after the oxidation of  $[\text{Tc}(\text{NO})(\text{NH}_3)_4\text{F}]^+$ , are well-reflected by the computational results. This mainly concerns the lengthening of the Tc–NO bond, which goes along with a shortening of the N–O bond as the result of reduced back-donation into an antibonding orbital. But also the experimentally detected shortening of the Tc– $\text{NH}_3$  and the Tc–F bonds is well-reproduced by the calculations. The latter effect, which is frequently described as “structural trans influence” due to the bonding of ligands in trans position to multiply bonded atoms, cannot easily be attributed to steric factors in the complexes under study, since neither the X-ray nor the computational data report any change in the (NO)–Tc–( $\text{NH}_3$ ) angles as a consequence of the oxidation. Thus, the observed shortening of the Tc–F bonds are determined electronically.

As shown by the reactions described above, the novel nitrosyltechnetium complexes are remarkably inert against ligand-exchange reactions. This is not unexpected for Tc(I) compounds with  $d^6$  configuration (and has been reported before for the related aqua complex  $[\text{Tc}(\text{NO})(\text{NH}_3)_4(\text{H}_2\text{O})]^{2+}$ ),<sup>56</sup> but a similar behavior of the Tc(II) compounds is unusual and in contrast to reports in previous studies in which the ammine ligands of  $[\text{Tc}(\text{NO})(\text{NH}_3)_4(\text{H}_2\text{O})]^{3+}$  are readily replaced by  $\text{Cl}^-$ <sup>40</sup> or in which halide exchange reactions in  $[\text{Tc}(\text{NO})\text{Cl}_n\text{Br}_{4-n}]^-$  complexes ( $n = 0\text{--}4$ ) are observed under mild conditions.<sup>49</sup> A noticeable

Scheme 4. Synthesis of  $[\text{Tc}(\text{NO})(\text{NH}_3)_4(\text{OOCF}_3)](\text{OOCF}_3)$ 

feature of the compounds reported in the present Paper is the presence of a fluorido ligand in trans position to  $\text{NO}^+$ . It obviously resists even reactions under drastic conditions such as heating in neat py. An exchange of the  $\text{F}^-$  ligand of  $[\text{Tc}(\text{NO})(\text{NH}_3)_4\text{F}](\text{HF}_2)$  under comparatively mild conditions was achieved during an attempted recrystallization from  $\text{CF}_3\text{COOH}$  at room temperature (Scheme 4).

Dissolution of  $[\text{Tc}(\text{NO})(\text{NH}_3)_4\text{F}](\text{HF}_2) \cdot 1/2\text{RbF}$  in trifluoroacetic acid and slow evaporation of the resulting clear solution gives orange-red crystals of  $[\text{Tc}(\text{NO})(\text{NH}_3)_4(\text{OOCF}_3)](\text{OOCF}_3) \cdot \text{CF}_3\text{COOH}$  in almost quantitative yield, while a similar procedure starting from  $[\text{Tc}(\text{NO})(\text{NH}_3)_4(\text{H}_2\text{O})]\text{Cl}_2$  only resulted in an anion exchange and the formation of  $[\text{Tc}(\text{NO})(\text{NH}_3)_4(\text{H}_2\text{O})](\text{CF}_3\text{COO})_2$ .<sup>36</sup>

The compound is soluble in common organic solvents such as acetone, ethanol, acetonitrile, tetrahydrofuran, or dichloromethane. Its IR spectrum shows the  $\text{N}=\text{O}$  stretch at  $1670\text{ cm}^{-1}$ . This value is close to the  $\text{N}=\text{O}$  stretches observed for the other Tc(I) compounds of the present study. IR bands of the coordinated  $\text{NH}_3$  are found at  $829$ ,  $1421$ , and  $1656\text{ cm}^{-1}$ . The Tc–NO vibration gives a band at  $614\text{ cm}^{-1}$ .

The  $^{99}\text{Tc}$  NMR spectrum of the diamagnetic  $[\text{Tc}(\text{NO})(\text{NH}_3)_4(\text{OOCF}_3)]^+$  cation shows a signal at  $2017\text{ ppm}$  ( $\Delta\nu_{1/2} = 3840\text{ Hz}$ ). This value is downfield-shifted by about  $90\text{ ppm}$  with respect to the values found for the salts containing the  $[\text{Tc}(\text{NO})(\text{NH}_3)_4\text{F}]^+$  cation ( $1926$ – $1933\text{ ppm}$ ). The reason for this shift as well as the range of the  $^{99}\text{Tc}$  chemical shifts may be subject of future considerations when more data are available.

$[\text{Tc}(\text{NO})(\text{NH}_3)_4(\text{OOCF}_3)](\text{OOCF}_3) \cdot \text{CF}_3\text{COOH}$  crystallizes in the triclinic space group  $P\bar{1}$ . The structure consists of a distorted octahedral  $[\text{Tc}(\text{NO})(\text{NH}_3)_4(\text{OOCF}_3)]^+$  cation and a  $\text{CF}_3\text{COO}^-$  anion. One molecule of  $\text{CF}_3\text{COOH}$  is cocrystallized. The molecular structure of the complex cation is shown in Figure 9. Selected bond lengths and angles are summarized in Table 6.

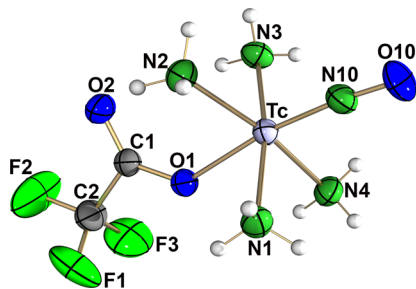


Figure 9. Ellipsoid plot of the complex anion of  $[\text{Tc}(\text{NO})(\text{NH}_3)_4(\text{OOCF}_3)](\text{OOCF}_3) \cdot \text{CF}_3\text{COOH}$ .<sup>34</sup>

The value of the Tc–NO bond length of  $1.720(3)\text{ \AA}$  is close to that observed for other nitrosyl complexes. The equatorial coordination sphere is occupied by the four ammine ligands,

Table 6. Selected Bond Lengths ( $\text{\AA}$ ) and Angles ( $\text{deg}$ ) in  $[\text{Tc}(\text{NO})(\text{NH}_3)_4(\text{OOCF}_3)](\text{OOCF}_3) \cdot \text{CF}_3\text{COOH}$

Tc–N10	1.720(3)	Tc1–N4	2.165(2)
N10–O10	1.194(4)	Tc1–O1	2.116(2)
Tc–N1	2.160(2)	C1–O1	1.260(3)
Tc–N2	2.161(2)	C1–O2	1.219(4)
Tc–N3	2.162(2)	C1–C2	1.541(4)
Tc–N10–O10	174.6(3)	N10–Tc–N2	96.5(1)
N10–Tc–O1	172.1(1)	N10–Tc–N3	97.5(1)
N10–Tc–N1	92.26(1)	N10–Tc–N4	93.2(1)

and the trifluoroacetato ligand is coordinated in a trans position to the nitrosyl ligand. The overall bonding situation is very similar to that in the  $[\text{Tc}(\text{NO})(\text{NH}_3)_4\text{F}]^+$  cation: a linear coordination of the nitrosyl ligand and a roof effect, which results in  $\text{N10–Tc–NH}_3$  angles all being larger than  $90^\circ$ . The Tc–O bond length to the *trans*-trifluoroacetato ligand is  $2.116(2)\text{ \AA}$ . This value is relatively long and similar to the value observed for the  $[\text{Ru}(\text{NH}_3)_4(\text{SO}_2)(\text{OOCF}_3)]^+$  cation ( $2.059\text{ \AA}$ ).<sup>61</sup> The carboxylate group is clearly monodentate, with the nonbonded oxygen atom being  $3.49\text{ \AA}$  away from the metal ion but with almost equal C1–O1 and C1–O2 bond lengths.

Several hydrogen bonds stabilize the solid-state structure of  $[\text{Tc}(\text{NO})(\text{NH}_3)_4(\text{OOCF}_3)](\text{OOCF}_3) \cdot \text{CF}_3\text{COOH}$ . Supporting Information, Figure S7 illustrates the hydrogen-bonding situation in the unit cell of the structure. A complete summary is given in Supporting Information, Table S7. The ammine ligands form a complex  $\text{N–H}\cdots\text{F}$  and  $\text{N–H}\cdots\text{O}$  network with the counterions and adjacent molecules, respectively.

## CONCLUSIONS

Haha is a suitable agent for the synthesis of low-valent nitrosyl complexes of technetium with fluorido ligands. Such compounds were hitherto not accessible by ligand-exchange protocols from halide complexes or by direct syntheses with other nitrosylation agents, since the related reactions did not give sufficient exchange rates, and fluoride does not act as a reducing agent in reductive nitrosylation procedures.

The key compounds of this chemistry,  $[\text{Tc}(\text{NO})\text{F}_5]^{2-}$  and  $[\text{Tc}(\text{NO})(\text{NH}_3)_4\text{F}]^+$ , are formed in good yields directly from pertechnetate and are remarkably stable in aqueous solutions. They can act as starting materials of ongoing ligand-exchange procedures, which may open the door for an extended coordination chemistry of low-valent technetium complexes with fluorido ligands. More reactions, particularly such with organic ligands and organometallic approaches, are currently undertaken in our laboratory.

## ASSOCIATED CONTENT

### Supporting Information

Crystallographic data in CIF format. This material is available free of charge via the Internet at <http://pubs.acs.org>. Additional

information on the structure determinations has been deposited with the Cambridge Structural Database.

## AUTHOR INFORMATION

### Corresponding Author

\*E-mail: ulrich.abram@fu-berlin.de.

### Notes

The authors declare no competing financial interest.

## ACKNOWLEDGMENTS

This work was generously supported by the Graduate School (GK 1582) "Fluorine as a key element" of the Deutsche Forschungsgemeinschaft.

## REFERENCES

- (1) Hayton, T. W.; Legzdins, P.; Sharp, W. B. *Chem. Rev.* **2002**, *102*, 935.
- (2) Wright, A. M.; Hayton, T. W. *Comments Inorg. Chem.* **2012**, *33*, 207.
- (3) Riener, K.; Haslinger, S.; Raba, A.; Högerl, M. P.; Cokoja, M.; Herrmann, W. A.; Kühn, F. E. *Chem. Rev.* DOI: 10.1021/cr4006439.
- (4) Rathgeb, A.; Böhm, A.; Novak, M. S.; Gavriluta, A.; Dömötör, O.; Tommasino, J. B.; Enyedy, E. A.; Shova, S.; Meier, S.; Jakupec, M. A.; Luneau, D.; Arion, V. B. *Inorg. Chem.* **2014**, *53*, 2718.
- (5) Rattat, D.; Schubiger, P. A.; Berke, H. G.; Schmalte, H.; Alberto, R. *Cancer Biother. Radiopharm.* **2001**, *16*, 339.
- (6) Rattat, D.; Verbruggen, A.; Schmalte, H.; Berke, H.; Alberto, R. *Tetrahedron Lett.* **2004**, *45*, 4089.
- (7) Rattat, D.; Verbruggen, A.; Berke, H.; Alberto, R. *J. Organomet. Chem.* **2004**, *689*, 4833.
- (8) Schibli, R.; Marti, N.; Maurer, P.; Spingler, B.; Lehaire, M.-L.; Gramlich, V.; Barnes, C. L. *Inorg. Chem.* **2005**, *44*, 683.
- (9) Rattat, D.; Verbruggen, A.; Berke, H. *Z. Anorg. Allg. Chem.* **2006**, *632*, 1351.
- (10) Balasekaran, S. M.; Molski, M.; Hagenbach, A.; Abram, U. *Z. Anorg. Allg. Chem.* **2013**, *639*, 672.
- (11) Balasekaran, S. M.; Molski, M.; Spandl, J.; Hagenbach, A.; Alberto, R.; Abram, U. *Inorg. Chem.* **2013**, *52*, 7094.
- (12) Alberto, R. *Technetium in Comprehensive Coordination Chemistry*; McCleverty, J. A., Meyer, T. J., Eds.; Elsevier: Amsterdam, Netherlands, 2005, Vol. 5, p 127.
- (13) Orvig, C.; Davison, A.; Jones, A. G. *J. Labelled Compd. Radiopharm.* **1981**, *18*, 148.
- (14) Brown, D. S.; Newman, J. S.; Thornback, J. R.; Davison, A. *Acta Crystallogr.* **1987**, *C43*, 1692.
- (15) Eakins, J. D.; Humphreys, D. G.; Mellish, C. E. *J. Chem. Soc.* **1963**, 6012.
- (16) Abram, U.; Kirmse, R.; Köhler, K.; Lorenz, B.; Kaden, L. *Inorg. Chim. Acta* **1987**, *129*, 15.
- (17) Pearlstein, R. M.; Davis, W. M.; Jones, A. G.; Davison, A. *Inorg. Chem.* **1989**, *28*, 3332.
- (18) Baldas, J.; Boas, J. F.; Bonnyman, J.; Williams, G. A. *J. Chem. Soc., Dalton Trans.* **1984**, 827.
- (19) Nicholson, T.; Müller, P.; Davison, A.; Jones, A. G. *Inorg. Chim. Acta* **2006**, *359*, 1296.
- (20) Kirmse, R.; Lorenz, B.; Schmidt, K. *Polyhedron* **1983**, *2*, 935.
- (21) Linder, K. E.; Davison, A.; Dean, J. C.; Costello, C. E.; Maleknia, S. *Inorg. Chem.* **1986**, *5*, 2085.
- (22) Gong, C.-M. S.; Lukens, W. W.; Poineau, F.; Czerwinski, K. R. *Inorg. Chem.* **2008**, *47*, 6674.
- (23) Chung, D. Y.; Lee, E. H. *J. Ind. Eng. Chem.* **2006**, *12*, 962.
- (24) Nevissi, A. E.; Silverston, M.; Strebin, R. S.; Kaye, J. H. *J. Radioanal. Nucl. Chem.* **1994**, *177*, 91.
- (25) Hahn, Th.; Klapper, H. Chapter 3.3. In *International Tables for Crystallography*; Wiley: Hoboken, NJ, 2006; Vol. D, p 393.
- (26) *Gaussian 09*, Revision C.01; Gaussian, Inc.: Wallingford, CT, 2009.
- (27) Vosko, S. H.; Wilk, L.; Nusair, W. *Can. J. Phys.* **1980**, *58*, 1200.
- (28) Lee, C.; Yang, W.; Parr, R. G. *Phys. Rev. B: Condens. Matter* **1988**, *37*, 785.
- (29) Becke, A. D. *J. Chem. Phys.* **1993**, *98*, 5648.
- (30) Raghavachari, K.; Binkley, J. S.; Seeger, R.; Pople, J. A. *J. Chem. Phys.* **1980**, *72*, 650.
- (31) Andrae, D.; Häußermann, U.; Dolg, M.; Stoll, H.; Preuß, H. *Theor. Chim. Acta* **1990**, *77*, 123.
- (32) Reed, A. E.; Curtis, L. A.; Weinhold, F. *Chem. Rev.* **1988**, *88*, 899.
- (33) Salomov, A. S.; Mikhailov, Y. N.; Kanishcheva, A. S.; Svetlov, A. A.; Sinitsyn, N. M.; Poraikoshits, M. A.; Parpiev, N. A. *Zh. Neorg. Khim.* **1989**, *34*, 386.
- (34) Brandenburg, K. *DIAMOND—a program for the visualization of crystal structures*, Vers. 3.2i; Crystal Impact GbR: Bonn, Germany, 2012.
- (35) Rogalevich, N. L.; Bobkova, E. Y.; Novitskii, G. G.; Skutov, I. K.; Svetlov, A. A.; Sinitsyn, N. M. *Zh. Neorg. Khim.* **1986**, *31*, 1221.
- (36) Reese, I.; Preetz, W. *Z. Anorg. Allg. Chem.* **2000**, *626*, 645.
- (37) Bouteiller, Y.; Gillet, J.-C.; Gregoire, G.; Schermann, J. P. *J. Phys. Chem.* **2008**, *112*, 11656.
- (38) Paulat, F.; Kuschel, T.; Näther, C.; Praneeth, V. K. K.; Sander, O.; Lehnert, N. *Inorg. Chem.* **2004**, *43*, 6979.
- (39) Kirmse, R.; Abram, U. *Isotopenpraxis* **1990**, *26*, 151.
- (40) Yang, G. C.; Heitzmann, M. W.; Ford, L. A.; Benson, W. R. *Inorg. Chem.* **1982**, *21*, 3242.
- (41) Kirmse, R.; Stach, J.; Lorenz, B.; Marov, I. N. *Z. Chem.* **1984**, *24*, 36.
- (42) Kirmse, R.; Stach, J.; Abram, U. *Polyhedron* **1985**, *4*, 1275.
- (43) Baldas, J.; Boas, J. F.; Bonnyman, J.; Williams, G. A. *J. Chem. Soc., Dalton Trans.* **1984**, 827.
- (44) Manoharan, P. T.; Rogers, M. T. *J. Chem. Phys.* **1968**, *49*, 5510.
- (45) Shock, J. R.; Rogers, M. T. *J. Chem. Phys.* **1973**, *58*, 3356.
- (46) Holloway, J. H.; Raynor, J. B. *J. Chem. Soc., Dalton Trans.* **1975**, 737.
- (47) Baldas, J.; Boas, J. F.; Colmanet, S. F.; Ivanov, Z.; Williams, G. A. *Radiochim. Acta* **1993**, *63*, 111.
- (48) Nicholson, T.; Kramer, D. J.; Davison, A.; Jones, A. G. *Inorg. Chim. Acta* **2001**, *316*, 110.
- (49) Kirmse, R.; Stach, J.; Abram, U.; Marov, I. N. *Z. Anorg. Allg. Chem.* **1984**, *518*, 210.
- (50) Schoemaker, D. *Phys. Rev. B* **1973**, *7*, 786.
- (51) Blanchard, S. S.; Nicholson, T.; Davison, A.; Davis, W.; Jones, A. G. *Inorg. Chim. Acta* **1996**, *244*, 121.
- (52) O'Connell, L. A.; Pearlstein, R. M.; Davison, A.; Thornback, J. R.; Kronauge, J. F.; Jones, A. G. *Inorg. Chim. Acta* **1989**, *161*, 39.
- (53) Mikhalev, V. A. *Radiochemistry* **2005**, *47*, 319.
- (54) Farrugia, L. J. *J. Appl. Crystallogr.* **2012**, *45*, 849.
- (55) Kimura, T.; Sakurai, T.; Shima, M.; Togano, T.; Mukaida, M.; Nomura, T. *Inorg. Chim. Acta* **1983**, *69*, 135.
- (56) Armstrong, R. A.; Taube, H. *Inorg. Chem.* **1976**, *15*, 1904.
- (57) Rush, J. J.; Schroeder, L. W.; Melveger, A. J. *J. Chem. Phys.* **1972**, *56*, 2793.
- (58) Nicholson, T.; Mahmood, A.; Refosco, F.; Tisato, F.; Müller, P.; Jones, A. G. *Inorg. Chim. Acta* **2009**, *362*, 3637.
- (59) Radonovich, L. J.; Hoard, J. L. *J. Phys. Chem.* **1984**, *88*, 6711.
- (60) Lu, J.; Clarke, M. J. *J. Chem. Soc., Dalton Trans.* **1992**, 1243.
- (61) Kovalevsky, A. Y.; Bagley, K. A.; Cole, J. M.; Coppens, P. *Inorg. Chem.* **2003**, *42*, 140.